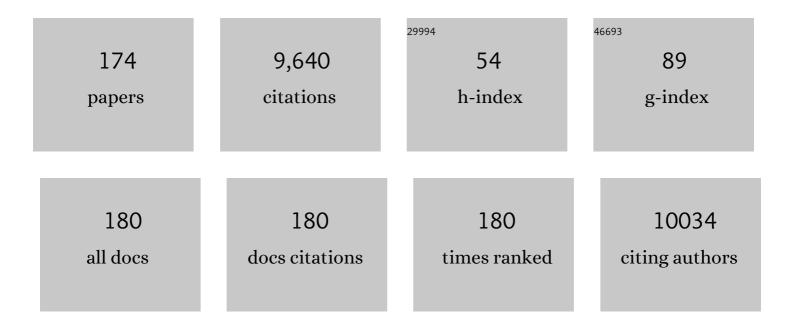
## José M Valpuesta

List of Publications by Year in descending order

Source: https://exaly.com/author-pdf/1181900/publications.pdf Version: 2024-02-01



#	Article	lF	CITATIONS
1	The Molecular Chaperone CCT Sequesters Gelsolin and Protects it from Cleavage by Caspase-3. Journal of Molecular Biology, 2022, 434, 167399.	2.0	5
2	Structural mechanism for tyrosine hydroxylase inhibition by dopamine and reactivation by Ser40 phosphorylation. Nature Communications, 2022, 13, 74.	5.8	23
3	Chaperonin Mechanisms: Multiple and (Mis)Understood?. Annual Review of Biophysics, 2022, 51, 115-133.	4.5	15
4	Combining Electron Microscopy (EM) and Cross-Linking Mass Spectrometry (XL-MS) for Structural Characterization of Protein Complexes. Methods in Molecular Biology, 2022, 2420, 217-232.	0.4	0
5	Chaperonins: Nanocarriers with Biotechnological Applications. Nanomaterials, 2021, 11, 503.	1.9	4
6	Folding for the Immune Synapse: CCT Chaperonin and the Cytoskeleton. Frontiers in Cell and Developmental Biology, 2021, 9, 658460.	1.8	7
7	Globular Aggregates Stemming from the Self-Assembly of an Amphiphilic N-Annulated Perylene Bisimide in Aqueous Media. Nanomaterials, 2021, 11, 1457.	1.9	4
8	Assisted assembly of bacteriophage T7 core components for genome translocation across the bacterial envelope. Proceedings of the National Academy of Sciences of the United States of America, 2021, 118, .	3.3	10
9	T cell asymmetry and metabolic crosstalk can fine-tune immunological synapses. Trends in Immunology, 2021, 42, 649-653.	2.9	4
10	Truncation-Driven Lateral Association of α-Synuclein Hinders Amyloid Clearance by the Hsp70-Based Disaggregase. International Journal of Molecular Sciences, 2021, 22, 12983.	1.8	4
11	The chaperonin CCT controls T cell receptor–driven 3D configuration of centrioles. Science Advances, 2020, 6, .	4.7	23
12	Structural insights into the ability of nucleoplasmin to assemble and chaperone histone octamers for DNA deposition. Scientific Reports, 2019, 9, 9487.	1.6	8
13	Elevated levels of Secreted-Frizzled-Related-Protein 1 contribute to Alzheimer's disease pathogenesis. Nature Neuroscience, 2019, 22, 1258-1268.	7.1	48
14	Structural and functional analysis of the role of the chaperonin CCT in mTOR complex assembly. Nature Communications, 2019, 10, 2865.	5.8	47
15	The cochaperone CHIP marks Hsp70- and Hsp90-bound substrates for degradation through a very flexible mechanism. Scientific Reports, 2019, 9, 5102.	1.6	38
16	Molecular architecture of the Bardet–Biedl syndrome protein 2-7-9 subcomplex. Journal of Biological Chemistry, 2019, 294, 16385-16399.	1.6	9
17	Engineering protein assemblies with allosteric control via monomer fold-switching. Nature Communications, 2019, 10, 5703.	5.8	17
18	The chaperonin CCT promotes the formation of fibrillar aggregates of Î <sup>3</sup> -tubulin. Biochimica Et Biophysica Acta - Proteins and Proteomics, 2018, 1866, 519-526.	1.1	22

José M Valpuesta

#	Article	IF	CITATIONS
19	Hsp70 chaperone: a master player in protein homeostasis. F1000Research, 2018, 7, 1497.	0.8	103
20	Structure and Function of the Cochaperone Prefoldin. Advances in Experimental Medicine and Biology, 2018, 1106, 119-131.	0.8	20
21	Expression, Functional Characterization, and Preliminary Crystallization of the Cochaperone Prefoldin from the Thermophilic Fungus Chaetomium thermophilum. International Journal of Molecular Sciences, 2018, 19, 2452.	1.8	4
22	The chaperonin CCT inhibits assembly of α-synuclein amyloid fibrils by a specific, conformation-dependent interaction. Scientific Reports, 2017, 7, 40859.	1.6	48
23	Domain topology of human Rasal. Biological Chemistry, 2017, 399, 63-72.	1.2	2
24	Hsp70 – a master regulator in protein degradation. FEBS Letters, 2017, 591, 2648-2660.	1.3	176
25	Structural characterization of the NAP; the major adhesion complex of the human pathogen <i>Mycoplasma genitalium</i> . Molecular Microbiology, 2017, 105, 869-879.	1.2	24
26	Identification of Key Amino Acid Residues Modulating Intracellular and In vitro Microcin E492 Amyloid Formation. Frontiers in Microbiology, 2016, 7, 35.	1.5	25
27	Molecular chaperones: functional mechanisms and nanotechnological applications. Nanotechnology, 2016, 27, 324004.	1.3	9
28	Clathrin-coat disassembly illuminates the mechanisms of Hsp70 force generation. Nature Structural and Molecular Biology, 2016, 23, 821-829.	3.6	67
29	Beyond the known functions of the CCR4â€NOT complex in gene expression regulatory mechanisms. BioEssays, 2016, 38, 1048-1058.	1.2	15
30	High resolution atomic force microscopy of double-stranded RNA. Nanoscale, 2016, 8, 11818-11826.	2.8	42
31	The architecture of the Schizosaccharomyces pombe CCR4-NOT complex. Nature Communications, 2016, 7, 10433.	5.8	47
32	The structure of the TBCE/TBCB chaperones and α-tubulin complex shows a tubulin dimer dissociation mechanism. Journal of Cell Science, 2015, 128, 1824-34.	1.2	27
33	Structures of the Gβ-CCT and PhLP1–Gβ-CCT complexes reveal a mechanism for G-protein β-subunit folding and Gβγ dimer assembly. Proceedings of the National Academy of Sciences of the United States of America, 2015, 112, 2413-2418.	3.3	49
34	Electron microscopy: the coming of age of a structural biology technique. Archives of Biochemistry and Biophysics, 2015, 581, 1-2.	1.4	3
35	Modulation of the Chaperone DnaK Allosterism by the Nucleotide Exchange Factor GrpE. Journal of Biological Chemistry, 2015, 290, 10083-10092.	1.6	20
36	Arc is a flexible modular protein capable of reversible self-oligomerization. Biochemical Journal, 2015, 468, 145-158.	1.7	69

3

#	Article	IF	CITATIONS
37	Structural characterization of toxic oligomers that are kinetically trapped during α-synuclein fibril formation. Proceedings of the National Academy of Sciences of the United States of America, 2015, 112, E1994-2003.	3.3	384
38	Dynamics, flexibility, and allostery in molecular chaperonins. FEBS Letters, 2015, 589, 2522-2532.	1.3	83
39	Mechano-chemical kinetics of DNA replication: identification of the translocation step of a replicative DNA polymerase. Nucleic Acids Research, 2015, 43, 3643-3652.	6.5	48
40	Phosphoinositide 3-Kinase Beta Protects Nuclear Envelope Integrity by Controlling RCC1 Localization and Ran Activity. Molecular and Cellular Biology, 2015, 35, 249-263.	1.1	12
41	Assisted protein folding at low temperature: evolutionary adaptation of the Antarctic fish chaperonin CCT and its client proteins. Biology Open, 2014, 3, 261-270.	0.6	12
42	Phosphorylation Dependence and Stoichiometry of the Complex Formed by Tyrosine Hydroxylase and 14-3-3γ. Molecular and Cellular Proteomics, 2014, 13, 2017-2030.	2.5	19
43	The intrinsically disordered distal face of nucleoplasmin recognizes distinct oligomerization states of histones. Nucleic Acids Research, 2014, 42, 1311-1325.	6.5	17
44	Yeast mitochondrial RNAP conformational changes are regulated by interactions with the mitochondrial transcription factor. Nucleic Acids Research, 2014, 42, 11246-11260.	6.5	7
45	Modulation of the Hsp90 Chaperone Cycle by a Stringent Client Protein. Molecular Cell, 2014, 53, 941-953.	4.5	129
46	Programmed Cell Death Protein 5 Interacts with the Cytosolic Chaperonin Containing Tailless Complex Polypeptide 1 (CCT) to Regulate β-Tubulin Folding. Journal of Biological Chemistry, 2014, 289, 4490-4502.	1.6	31
47	Molecular determinants of the ATP hydrolysis asymmetry of the CCT chaperonin complex. Proteins: Structure, Function and Bioinformatics, 2014, 82, 703-707.	1.5	21
48	Structural characterization of the substrate transfer mechanism in Hsp70/Hsp90 folding machinery mediated by Hop. Nature Communications, 2014, 5, 5484.	5.8	104
49	Identification of the Translocation Step of a Replicative DNA Polymerase. Biophysical Journal, 2014, 106, 229a.	0.2	Ο
50	Structural Characterization of the Bacteriophage T7 Tail Machinery. Journal of Biological Chemistry, 2013, 288, 26290-26299.	1.6	75
51	Mechanical Identities of RNA and DNA Double Helices Unveiled at the Single-Molecule Level. Journal of the American Chemical Society, 2013, 135, 122-131.	6.6	139
52	Interaction of p53 with the CCT Complex Promotes Protein Folding and Wild-Type p53 Activity. Molecular Cell, 2013, 50, 805-817.	4.5	121
53	Segregated ordered lipid phases and protein-promoted membrane cohesivity are required for pulmonary surfactant films to stabilize and protect the respiratory surface. Faraday Discussions, 2013, 161, 535-548.	1.6	57
54	Structural Insights into the Chaperone Activity of the 40-kDa Heat Shock Protein DnaJ. Journal of Biological Chemistry, 2013, 288, 15065-15074.	1.6	21

#	Article	IF	CITATIONS
55	Microcin E492 Amyloid Formation Is Retarded by Posttranslational Modification. Journal of Bacteriology, 2013, 195, 3995-4004.	1.0	31
56	Phosphoinositide 3-kinase beta controls replication factor C assembly and function. Nucleic Acids Research, 2013, 41, 855-868.	6.5	6
57	Large Terminase Conformational Change Induced by Connector Binding in Bacteriophage T7. Journal of Biological Chemistry, 2013, 288, 16998-17007.	1.6	33
58	Structure and Non-Structure of Centrosomal Proteins. PLoS ONE, 2013, 8, e62633.	1.1	25
59	Architecture and nucleic acids recognition mechanism of the THO complex, an mRNP assembly factor. EMBO Journal, 2012, 31, 1605-1616.	3.5	79
60	The yeast THO complex forms a 5-subunit assembly that directly interacts with active chromatin. Bioarchitecture, 2012, 2, 134-137.	1.5	14
61	Manipulation of single polymerase-DNA complexes: A mechanical view of DNA unwinding during replication. Cell Cycle, 2012, 11, 2967-2968.	1.3	9
62	The Hexameric Structure of a Conjugative VirB4 Protein ATPase Provides New Insights for a Functional and Phylogenetic Relationship with DNA Translocases. Journal of Biological Chemistry, 2012, 287, 39925-39932.	1.6	66
63	Active DNA unwinding dynamics during processive DNA replication. Proceedings of the National Academy of Sciences of the United States of America, 2012, 109, 8115-8120.	3.3	67
64	The Structure of Native Influenza Virion Ribonucleoproteins. Science, 2012, 338, 1634-1637.	6.0	254
65	Structural characterization of microcin E492 amyloid formation: Identification of the precursors. Journal of Structural Biology, 2012, 178, 54-60.	1.3	22
66	Mechanical stability of lowâ€humidity single DNA molecules. Biopolymers, 2012, 97, 199-208.	1.2	13
67	Recognition of Membrane-Bound Fusion-Peptide/MPER Complexes by the HIV-1 Neutralizing 2F5 Antibody: Implications for Anti-2F5 Immunogenicity. PLoS ONE, 2012, 7, e52740.	1.1	9
68	Condensation Prevails over B-A Transition in the Structure of DNA at Low Humidity. Biophysical Journal, 2011, 100, 2006-2015.	0.2	33
69	Mechanical Properties of High-Gâ‹C Content DNA with A-Type Base-Stacking. Biophysical Journal, 2011, 100, 1996-2005.	0.2	20
70	Dna Unwinding Dynamics of a Processive DNA Polymerase. Biophysical Journal, 2011, 100, 239a.	0.2	0
71	Increased Sensitivity of Antigen-Experienced T Cells through the Enrichment of Oligomeric T Cell Receptor Complexes. Immunity, 2011, 35, 375-387.	6.6	153
72	Crystal structure of the open conformation of the mammalian chaperonin CCT in complex with tubulin. Nature Structural and Molecular Biology, 2011, 18, 14-19.	3.6	128

#	Article	IF	CITATIONS
73	Chaperonins: two rings for folding. Trends in Biochemical Sciences, 2011, 36, 424-432.	3.7	140
74	Molecular Rearrangements Involved in the Capsid Shell Maturation of Bacteriophage T7. Journal of Biological Chemistry, 2011, 286, 234-242.	1.6	55
75	Characterization of the structure and self-recognition of the human centrosomal protein NA14: implications for stability and function. Protein Engineering, Design and Selection, 2011, 24, 883-892.	1.0	7
76	Bacterial Tubulin Distinct Loop Sequences and Primitive Assembly Properties Support Its Origin from a Eukaryotic Tubulin Ancestor. Journal of Biological Chemistry, 2011, 286, 19789-19803.	1.6	35
77	Prefoldin 5 Is Required for Normal Sensory and Neuronal Development in a Murine Model. Journal of Biological Chemistry, 2011, 286, 726-736.	1.6	45
78	Size-selective recognition of gold nanoparticles by a molecular chaperone. Chemical Physics Letters, 2010, 501, 108-112.	1.2	8
79	Structural characterization of the TCR complex by electron microscopy. International Immunology, 2010, 22, 897-903.	1.8	19
80	Structure of GroEL in Complex with an Early Folding Intermediate of Alanine Glyoxylate Aminotransferase. Journal of Biological Chemistry, 2010, 285, 6371-6376.	1.6	19
81	Nucleoplasmin Binds Histone H2A-H2B Dimers through Its Distal Face*. Journal of Biological Chemistry, 2010, 285, 33771-33778.	1.6	29
82	Structural Analysis of the Interactions Between Hsp70 Chaperones and the Yeast DNA Replication Protein Orc4p. Journal of Molecular Biology, 2010, 403, 24-39.	2.0	11
83	The Structure of a Biologically Active Influenza Virus Ribonucleoprotein Complex. PLoS Pathogens, 2009, 5, e1000491.	2.1	186
84	A new side opening on prolyl oligopeptidase revealed by electron microscopy. FEBS Letters, 2009, 583, 3344-3348.	1.3	17
85	SADB phosphorylation of γ-tubulin regulates centrosome duplication. Nature Cell Biology, 2009, 11, 1081-1092.	4.6	73
86	Single Centrosome Manipulation Reveals Its Electric Charge and Associated Dynamic Structure. Biophysical Journal, 2009, 97, 1022-1030.	0.2	22
87	Gold Nanoparticles Generated in Ethosome Bilayers, As Revealed by Cryo-Electron-Tomography. Journal of Physical Chemistry B, 2009, 113, 3051-3057.	1.2	25
88	α,γ-Peptide Nanotube Templating of One-Dimensional Parallel Fullerene Arrangements. Journal of the American Chemical Society, 2009, 131, 11335-11337.	6.6	81
89	The structure of CCT–Hsc70NBD suggests a mechanism for Hsp70 delivery of substrates to the chaperonin. Nature Structural and Molecular Biology, 2008, 15, 858-864.	3.6	85
90	Energetics and Geometry of FtsZ Polymers: Nucleated Self-Assembly of Single Protofilaments. Biophysical Journal, 2008, 94, 1796-1806.	0.2	100

#	Article	IF	CITATIONS
91	Structure of the Hsp110:Hsc70 Nucleotide Exchange Machine. Molecular Cell, 2008, 31, 232-243.	4.5	202
92	The Broadly Neutralizing Anti-Human Immunodeficiency Virus Type 1 4E10 Monoclonal Antibody Is Better Adapted to Membrane-Bound Epitope Recognition and Blocking than 2F5. Journal of Virology, 2008, 82, 8986-8996.	1.5	44
93	Sequential Action of ATP-dependent Subunit Conformational Change and Interaction between Helical Protrusions in the Closure of the Built-in Lid of Group II Chaperonins. Journal of Biological Chemistry, 2008, 283, 34773-34784.	1.6	24
94	The interâ€ring arrangement of the cytosolic chaperonin CCT. EMBO Reports, 2007, 8, 252-257.	2.0	37
95	Divergent Substrate-Binding Mechanisms Reveal an Evolutionary Specialization of Eukaryotic Prefoldin Compared to Its Archaeal Counterpart. Structure, 2007, 15, 101-110.	1.6	55
96	The three-dimensional structure of an eukaryotic glutamine synthetase: Functional implications of its oligomeric structure. Journal of Structural Biology, 2006, 156, 469-479.	1.3	61
97	All three chaperonin genes in the archaeon Haloferax volcanii are individually dispensable. Molecular Microbiology, 2006, 61, 1583-1597.	1.2	31
98	PhLP3 Modulates CCT-mediated Actin and Tubulin Folding via Ternary Complexes with Substrates. Journal of Biological Chemistry, 2006, 281, 7012-7021.	1.6	69
99	lonic interactions at both inter-ring contact sites of GroEL are involved in transmission of the allosteric signal: A time-resolved infrared difference study. Protein Science, 2005, 14, 2267-2274.	3.1	8
100	Maturation of phage T7 involves structural modification of both shell and inner core components. EMBO Journal, 2005, 24, 3820-3829.	3.5	118
101	Coexistence of multivalent and monovalent TCRs explains high sensitivity and wide range of response. Journal of Experimental Medicine, 2005, 202, 493-503.	4.2	288
102	Folding, Stability and Polymerization Properties of FtsZ Chimeras with Inserted Tubulin Loops Involved in the Interaction with the Cytosolic Chaperonin CCT and in Microtubule Formation. Journal of Molecular Biology, 2005, 346, 319-330.	2.0	13
103	Structure of the Connector of Bacteriophage T7 at 8Ã Resolution: Structural Homologies of a Basic Component of a DNA Translocating Machinery. Journal of Molecular Biology, 2005, 347, 895-902.	2.0	99
104	Structure of the complex between the cytosolic chaperonin CCT and phosducin-like protein. Proceedings of the National Academy of Sciences of the United States of America, 2004, 101, 17410-17415.	3.3	65
105	Molecular clamp mechanism of substrate binding by hydrophobic coiled-coil residues of the archaeal chaperone prefoldin. Proceedings of the National Academy of Sciences of the United States of America, 2004, 101, 4367-4372.	3.3	57
106	3D structure of the influenza virus polymerase complex: Localization of subunit domains. Proceedings of the National Academy of Sciences of the United States of America, 2004, 101, 308-313.	3.3	116
107	The substrate recognition mechanisms in chaperonins. Journal of Molecular Recognition, 2004, 17, 85-94.	1.1	71
108	GroEL Stability and Function. Journal of Biological Chemistry, 2003, 278, 32083-32090.	1.6	24

#	Article	IF	CITATIONS
109	Assembly of Archaeal Cell Division Protein FtsZ and a GTPase-inactive Mutant into Double-stranded Filaments. Journal of Biological Chemistry, 2003, 278, 33562-33570.	1.6	86
110	Purification and Properties of TrwB, a Hexameric, ATP-binding Integral Membrane Protein Essential for R388 Plasmid Conjugation. Journal of Biological Chemistry, 2002, 277, 46456-46462.	1.6	63
111	Salt Bridges at the Inter-ring Interface Regulate the Thermostat of GroEL. Journal of Biological Chemistry, 2002, 277, 34024-34029.	1.6	21
112	Detailed architecture of a DNA translocating machine: the high-resolution structure of the bacteriophage φ29 connector particle 1 1Edited by R. Huber. Journal of Molecular Biology, 2002, 315, 663-676.	2.0	205
113	Structure and function of a protein folding machine: the eukaryotic cytosolic chaperonin CCT. FEBS Letters, 2002, 529, 11-16.	1.3	193
114	Note to the Paper by Guasch et al. (2002) Detailed Architecture of a DNA Translocating Machine: The High-resolution Structure of the Bacteriophage φ29 Connector Particle. Journal of Molecular Biology, 2002, 321, 379-380.	2.0	2
115	Structure of eukaryotic prefoldin and of its complexes with unfolded actin and the cytosolic chaperonin CCT. EMBO Journal, 2002, 21, 6377-6386.	3.5	184
116	Threeâ€dimensional reconstruction of a recombinant influenza virus ribonucleoprotein particle. EMBO Reports, 2001, 2, 313-317.	2.0	85
117	Analysis of the Interaction between the Eukaryotic Chaperonin CCT and Its Substrates Actin and Tubulin. Journal of Structural Biology, 2001, 135, 205-218.	1.3	70
118	Point Mutations in a Hinge Linking the Small and Large Domains of β-Actin Result in Trapped Folding Intermediates Bound to Cytosolic Chaperonin CCT. Journal of Structural Biology, 2001, 135, 198-204.	1.3	35
119	Chaperonins: Folding in the Hole. Journal of Structural Biology, 2001, 135, 83.	1.3	1
120	Characterization by atomic force microscopy and cryoelectron microscopy of tau polymers assembled in Alzheimer's disease1. Journal of Alzheimer's Disease, 2001, 3, 443-451.	1.2	14
121	HYDROMIC: prediction of hydrodynamic properties of rigid macromolecular structures obtained from electron microscopy images. European Biophysics Journal, 2001, 30, 457-462.	1.2	45
122	Structural comparison of prokaryotic and eukaryotic chaperonins. Micron, 2001, 32, 43-50.	1.1	43
123	The 'sequential allosteric ring' mechanism in the eukaryotic chaperonin-assisted folding of actin and tubulin. EMBO Journal, 2001, 20, 4065-4075.	3.5	130
124	Excluded Volume Effects on the Refolding and Assembly of an Oligomeric Protein. Journal of Biological Chemistry, 2001, 276, 957-964.	1.6	38
125	Purification and functional characterization of p16, the ATPase of the bacteriophage Phi29 packaging machinery. Nucleic Acids Research, 2001, 29, 4264-4273.	6.5	38
126	Eukaryotic chaperonin CCT stabilizes actin and tubulin folding intermediates in open quasi-native conformations. EMBO Journal, 2000, 19, 5971-5979.	3.5	193

#	Article	IF	CITATIONS
127	Partial Occlusion of Both Cavities of the Eukaryotic Chaperonin with Antibody Has No Effect upon the Rates of β-Actin or α-Tubulin Folding. Journal of Biological Chemistry, 2000, 275, 4587-4591.	1.6	31
128	Topology of the components of the DNA packaging machinery in the phage φ29 prohead. Journal of Molecular Biology, 2000, 298, 807-815.	2.0	70
129	Structural Analysis of the Bacteriophage T3 Head-to-Tail Connector. Journal of Structural Biology, 2000, 131, 146-155.	1.3	38
130	Interactions of the HIV-1 fusion peptide with large unilamellar vesicles and monolayers. A cryo-TEM and spectroscopic study. Biochimica Et Biophysica Acta - Biomembranes, 2000, 1467, 153-164.	1.4	36
131	Ultrastructural and Functional Analyses of Recombinant Influenza Virus Ribonucleoproteins Suggest Dimerization of Nucleoprotein during Virus Amplification. Journal of Virology, 2000, 74, 156-163.	1.5	111
132	Conformational Changes Generated in GroEL during ATP Hydrolysis as Seen by Time-resolved Infrared Spectroscopy. Journal of Biological Chemistry, 1999, 274, 5508-5513.	1.6	24
133	Characterization of ATP and DNA Binding Activities of TrwB, the Coupling Protein Essential in Plasmid R388 Conjugation. Journal of Biological Chemistry, 1999, 274, 36117-36124.	1.6	97
134	IHF protein inhibits cleavage but not assembly of plasmid R388 relaxosomes. Molecular Microbiology, 1999, 31, 1643-1652.	1.2	24
135	3D reconstruction of the ATP-bound form of CCT reveals the asymmetric folding conformation of a type II chaperonin. Nature Structural Biology, 1999, 6, 639-642.	9.7	102
136	Stress-induced recrystallization of a protein crystal by electron irradiation. Nature, 1999, 399, 51-54.	13.7	27
137	Eukaryotic type II chaperonin CCT interacts with actin through specific subunits. Nature, 1999, 402, 693-696.	13.7	247
138	Interbilayer lipid mixing induced by the human immunodeficiency virus type-1 fusion peptide on large unilamellar vesicles: the nature of the nonlamellar intermediates. Chemistry and Physics of Lipids, 1999, 103, 11-20.	1.5	31
139	The three-dimensional structure of a DNA translocating machine at 10 Ã resolution. Structure, 1999, 7, 289-296.	1.6	52
140	ATP hydrolysis induces an intermediate conformational state in GroEL. FEBS Journal, 1999, 259, 347-355.	0.2	10
141	Domain architecture of the bacteriophage Φ29 connector protein. Journal of Molecular Biology, 1999, 288, 899-909.	2.0	33
142	Selection of antibody probes to correlate protein sequence domains with their structural distribution. Protein Science, 1999, 8, 883-889.	3.1	22
143	Purification, crystallization and preliminary X-ray diffraction studies of the bacteriophage φ29 connector particle. FEBS Letters, 1998, 430, 283-287.	1.3	9
144	Crystallographic analysis reveals the 12-fold symmetry of the bacteriophage φ29 connector particle. Journal of Molecular Biology, 1998, 281, 219-225.	2.0	39

#	Article	IF	CITATIONS
145	ATP Binding Induces Large Conformational Changes in the Apical and Equatorial Domains of the Eukaryotic Chaperonin Containing TCP-1 Complex. Journal of Biological Chemistry, 1998, 273, 10091-10094.	1.6	54
146	Changes in Microtubule Protofilament Number Induced by Taxol Binding to an Easily Accessible Site. Journal of Biological Chemistry, 1998, 273, 33803-33810.	1.6	104
147	GroEL under Heat-Shock. Journal of Biological Chemistry, 1998, 273, 32587-32594.	1.6	49
148	Effects of the Inter-ring Communication in GroEL Structural and Functional Asymmetry. Journal of Biological Chemistry, 1997, 272, 32925-32932.	1.6	20
149	Conformational Changes in the GroEL Oligomer during the Functional Cycle. Journal of Structural Biology, 1997, 118, 31-42.	1.3	38
150	Symmetric GroEL-GroES complexes can contain substrate simultaneously in both GroEL rings. FEBS Letters, 1997, 405, 195-199.	1.3	33
151	Role of the amino terminal domain in GroES oligomerization. BBA - Proteins and Proteomics, 1997, 1337, 47-56.	2.1	6
152	The Interaction of DNA with Bacteriophage φ29 Connector: A Study by AFM and TEM. Journal of Structural Biology, 1996, 116, 390-398.	1.3	25
153	Biochemical Characterization of Symmetric GroEL-GroES Complexes. Journal of Biological Chemistry, 1996, 271, 68-76.	1.6	40
154	Polymerization of τ into Filaments in the Presence of Heparin: The Minimal Sequence Required for τ ―τ Interaction. Journal of Neurochemistry, 1996, 67, 1183-1190.	2.1	352
155	Prediction of the structure of GroES and its interaction with GroEL. Proteins: Structure, Function and Bioinformatics, 1995, 22, 199-209.	1.5	14
156	An intrinsic-tryptophan-fluorescence study of phage phi29 connector/nucleic acid interactions. FEBS Journal, 1994, 225, 747-753.	0.2	5
157	Reversible interaction of beta-actin along the channel of the TCP-1 cytoplasmic chaperonin. Biophysical Journal, 1994, 67, 364-368.	0.2	64
158	Analysis of Electron Microscope Images and Electron Diffraction Patterns of Thin Crystals of Ã~29 Connectors in Ice. Journal of Molecular Biology, 1994, 240, 281-287.	2.0	151
159	The formation of symmetrical GroEL-GroES complexes in the presence of ATP. FEBS Letters, 1994, 345, 181-186.	1.3	86
160	Structure and thermal denaturation of crystalline and noncrystalline cytochrome oxidase as studied by infrared spectroscopy. Biochemistry, 1994, 33, 11650-11655.	1.2	132
161	Structure of viral connectors and their function in bacteriophage assembly and DNA packaging. Quarterly Reviews of Biophysics, 1994, 27, 107-155.	2.4	157
162	A structural model for the GroEL chaperonin. FEMS Microbiology Letters, 1993, 106, 301-308.	0.7	7

José M Valpuesta

#	Article	IF	CITATIONS
163	DNA conformational change induced by the bacteriophage Φ29 connector. Nucleic Acids Research, 1992, 20, 5549-5554.	6.5	15
164	Three-dimensional structure of T3 connector purified from overexpressing bacteria. Journal of Molecular Biology, 1992, 224, 103-112.	2.0	45
165	An infrared spectroscopic study of specifically deuterated fatty-acyl methyl groups in phosphatidylcholine liposomes. Biochimica Et Biophysica Acta - Biomembranes, 1991, 1065, 29-34.	1.4	14
166	Infrared spectroscopic studies of detergent-solubilized uncoupling protein from brown-adipose-tissue mitochondria. FEBS Journal, 1990, 188, 83-89.	0.2	30
167	Electron cryo-microscopic analysis of crystalline cytochrome oxidase. Journal of Molecular Biology, 1990, 214, 237-251.	2.0	60
168	A Triton X-100-hydroxyapatite procedure for a rapid purification of bovine heart cytochrome-c oxidase. Characterization of the cytochrome-c oxidase/Triton X-100/phospholipid mixed micelles by laser light scattering. BBA - Proteins and Proteomics, 1988, 955, 371-375.	2.1	6
169	Lipid-protein interactions. The mitochondrial complex III-phosphatidylcholine-water system. Biochimica Et Biophysica Acta - Biomembranes, 1988, 942, 341-352.	1.4	10
170	Tryptophan fluorescence of mitochondrial complex III reconstituted in phosphatidylcholine bilayers. Archives of Biochemistry and Biophysics, 1987, 257, 285-292.	1.4	7
171	Laser light-scattering characterization of mitochondrial complex III-Triton X-100-phospholipid mixed micelles. Biochimica Et Biophysica Acta - Bioenergetics, 1985, 807, 96-99.	0.5	8
172	Physiological state of submitochondrial particles and their susceptibility to Triton X-100. Experientia, 1984, 40, 193-195.	1.2	0
173	Effect of the nonionic detergent Triton X-100 on mitochondrial succinate-oxidizing enzymes. Archives of Biochemistry and Biophysics, 1984, 228, 560-568.	1.4	20
174	Lipids of marine teleost fish (Teleostei). Biochemical Society Transactions, 1980, 8, 547-548.	1.6	0